[redacted]

NACA

RESEARCH MEMORANDUM

for the

U. S. Air Force

EXPERIMENTAL INVESTIGATION AT HIGH SUBSONIC SPEEDS OF THE ROLLING-STABILITY DERIVATIVES OF A 1/22-SCALE MODEL OF THE REPUBLIC F-105 AIRPLANE

By William C. Sleeman, Jr., and William C. Hayes, Jr.

Langley Aeronautical Laboratory
Langley Field, Va.

NATIONAL ADVISORY COMMITTEE
FOR AERONAUTICS

WASHINGTON

[redacted]

NACA RM SL55F16

NATIONAL ADVISORY COMMITTEE FOR AERONAUTICS

RESEARCH MEMORANDUM

for the

U. S. Air Force

EXPERIMENTAL INVESTIGATION AT HIGH SUBSONIC SPEEDS OF THE ROLLING-STABILITY DERIVATIVES OF A 1/22-SCALE MODEL OF THE REPUBLIC F-105 AIRPLANE

By William C. Sleeman, Jr., and William C. Hayes, Jr.

SUMMARY

Rolling-stability derivatives are presented for a 1/22-scale model of the Republic F-105 airplane over a Mach number range from 0.60 to 0.95 and for angles of attack up to approximately 13° at the lower Mach numbers. The model wing had an aspect ratio of 3.182 and a taper ratio of 0.467 and was swept back 45° at the quarter-chord line; the airfoil sections parallel to the model center line varied from NACA 65A005.5 at the 0.381-semispan station to NACA 65A003.7 at the wing tip. In addition to the data obtained for the complete model, rolling derivatives are also presented for three angles of attack for the model with the tail surfaces removed.

The results indicated that the model retained damping in roll (negative values of the derivative C_{l_p}) throughout the test ranges of Mach number and angle of attack; however, values of the damping varied considerably and at angles of attack of from 10° to 13° generally were about one-half as large as at zero angle of attack.

The derivatives of yawing moment and lateral force due to rolling generally followed trends indicated by previously published data on a general research model.

INTRODUCTION

The present investigation was undertaken at the request of the Air Force to provide information on the rolling-stability derivatives of

a 1/22-scale model of the Republic F-105 airplane. The technique used was similar to that employed in references 1 to 4.

Results were obtained in the Langley high-speed 7- by 10-foot tunnel for a Mach number range of 0.60 to 0.95 and for angles of attack up to approximately 13° at the lower Mach numbers by using the steady forced-roll testing technique. The data were obtained for the complete model configuration through ranges of angle of attack at various Mach numbers; however, data at only three angles of attack were obtained for the wing-fuselage configuration because difficulties with the tunnel drive system prevented completion of the test program.

COEFFICIENTS AND SYMBOLS

The results of this investigation are referred to the stability system of axes shown in figure 1, which shows the positive direction of forces, moments, and velocities. Moments are referred to the center-of-gravity location shown in figure 2 (at a longitudinal position corresponding to 25 percent mean aerodynamic chord and at a vertical position 5.71 percent mean aerodynamic chord above the fuselage center line).

C_L lift coefficient, $\frac{\text{Lift}}{qS}$

C_l rolling-moment coefficient, $\frac{\text{Rolling moment}}{qSb}$

C_n yawing-moment coefficient, $\frac{\text{Yawing moment}}{qSb}$

C_Y lateral-force coefficient, $\frac{\text{Lateral force}}{qS}$

S wing area, sq ft

b wing span, ft

$\bar{c}$ mean aerodynamic chord, ft

q dynamic pressure, $\frac{\rho V^2}{2}$, lb/sq ft

ρ mass density of air, slugs/cu ft

V free-stream velocity, ft/sec

M	Mach number
p	rolling velocity about X-axis of stability axes, radians/sec
pb/2V	wing-tip helix angle, radians
α	angle of attack of fuselage reference line, deg

$$C_{l_p} = \frac{\partial C_l}{\partial(pb/2V)}, \text{ per radian}$$

$$C_{n_p} = \frac{\partial C_n}{\partial(pb/2V)}, \text{ per radian}$$

$$C_{Y_p} = \frac{\partial C_Y}{\partial(pb/2V)}, \text{ per radian}$$

MODEL AND APPARATUS

The general arrangement of the 1/22-scale model of the Republic F-105 airplane is shown in figure 2 and some of the most pertinent geometric characteristics of the model are given in table I. Photographs of the model mounted on the forced-roll support system in the Langley high-speed 7- by 10-foot tunnel are given as figure 3. The steel wing had an aspect ratio of 3.182 and a taper ratio of 0.467 and was swept back 45° at the quarter-chord line; the airfoil sections parallel to the model center line varied from NACA 65A005.5 at the 0.381-semispan station to NACA 65A003.7 at the wing tip. The tail surfaces were made of aluminum and were swept back 45° at the quarter chord.

The model was tested in steady roll on the forced-roll sting support shown schematically in figure 4. For these tests, the model was mounted on a six-component internal strain-gage balance and was rotated about the X-axis of the stability axes system. Electrical signals from the strain-gage balance were transmitted to the data-recording equipment by means of wire leads, slip rings, and brushes. (See fig. 4.) The model angle of attack was changed by use of various offset sting adapters (figs. 3(b) and 4) which were designed to allow the model to rotate about the moment reference center at each angle of attack. Further details of the forced-roll testing technique can be found in reference 4.

TESTS AND CORRECTIONS

Tests were made in the Langley high-speed 7- by 10-foot tunnel over a Mach number range from 0.60 to 0.95 and through an angle-of-attack range from 0° to approximately 13°. The variations of mean test Reynolds number, based on the wing mean aerodynamic chord, and maximum wing-tip helix angle with Mach number are presented in figure 5. It should be noted that the maximum values of the wing-tip helix angle obtained in the tests were small because dynamic loads on the model limited the rolling velocity to approximately one-half of that normally obtainable with the test equipment.

Jet-boundary corrections applied to the angle of attack were determined from reference 5. Corrections for jet-boundary effects on rotary derivatives were not applied to the data inasmuch as these corrections are believed to be negligible for the relatively small model tested.

Blockage corrections applied to the Mach number and dynamic pressure were determined from reference 6.

The support system deflected under load and these deflections, combined with any initial displacement of the mass center of gravity of the model from the roll axis, introduced centrifugal forces and moments when the model was rotated. Corrections for these forces and moments have been applied to the data. The angles of attack have also been corrected for deflection of the model and support system under load.

Corrections for model wing distortion were assumed to be negligible.

RESULTS

The variation of lift coefficient with angle of attack as determined from the present tests is compared in figure 6 with unpublished results obtained on this model in the Langley 8-foot transonic tunnel. The values of lift coefficient for the rolling tests were obtained from a fairing of test data through $pb/2V = 0$ and these values are in excellent agreement with the static results presented in figure 6.

The basic data of this investigation were obtained as variations of forces and moments with wing-tip helix angle, and inasmuch as these variations were generally linear, the rolling derivatives rather than the basic data are presented herein (fig. 7). Data obtained from the tail-off configuration are presented for three angles of attack.

The damping-in-roll derivative C_{l_p} for both the complete and tail-off configurations increased with angle of attack up to about 4°, decreased at the higher angles up to about 12°, and then tended to increase again for Mach numbers above 0.60. This variation of damping in roll was consistent over the Mach number range to 0.90. For the test conditions, no reversed damping was indicated; although at angles of attack of from 10° to 13°, the magnitude of the damping generally was about one-half that at zero angle of attack.

The derivatives of yawing moment due to rolling C_{n_p} and lateral force due to rolling C_{Y_p} generally followed the trends indicated in reference 4 for angles of attack from 0° to 6°. The present data indicate rapidly increasing values of C_{n_p} as the highest test angle of attack (13°) is approached.

Test results pertaining to damping in roll obtained in this investigation are summarized in figure 8 for the test range of lift coefficient and Mach number. In figure 8, the losses in damping are indicated by the solid curve which shows combinations of lift coefficient and Mach number for which the damping in roll for lifting conditions has decreased to one-half the initial value of damping at zero lift.

Langley Aeronautical Laboratory,
National Advisory Committee for Aeronautics,
Langley Field, Va., June 9, 1955.

William C. Sleeman, Jr.
Aeronautical Research Scientist

William C. Hayes, Jr.
Aeronautical Research Scientist

Approved: Thomas A. Harris

Thomas A. Harris
Chief of Stability Research Division

dh

REFERENCES

1. Wiggins, James W.: Wind-Tunnel Investigation at High Subsonic Speeds To Determine the Rolling Derivatives of Two Wing-Fuselage Combinations Having Triangular Wings, Including a Semiempirical Method of Estimating the Rolling Derivatives. NACA RM L53L18a, 1954.

2. Wiggins, James W.: Wind-Tunnel Investigation of Effect of Sweep on Rolling Derivatives at Angles of Attack Up to 13° and at High Subsonic Mach Numbers, Including a Semiempirical Method of Estimating the Rolling Derivatives. NACA RM L54C26, 1954.

3. Sleeman, William C., Jr.: Experimental Investigation at High Subsonic Speeds To Determine the Rolling-Stability Derivatives of Three Wing-Fuselage Configurations. NACA RM L54H11, 1954.

4. Kuhn, Richard E., and Wiggins, James W.: Wind-Tunnel Investigation To Determine the Aerodynamic Characteristics in Steady Roll of a Model at High Subsonic Speeds. NACA RM L52K24, 1953.

5. Glauert, H.: The Elements of Aerofoil and Airscrew Theory. Second ed., Cambridge Univ. Press, 1947. (Reprinted 1948.)

6. Herriot, John G.: Blockage Corrections for Three-Dimensional-Flow Closed-Throat Wind Tunnels, With Consideration of the Effect of Compressibility. NACA Rep. 995, 1950. (Supersedes NACA RM A7B28.)

TABLE I

GEOMETRIC CHARACTERISTICS OF WING AND TAIL SURFACES

Wing:	
Span (theoretical), ft	1.591
Root chord (theoretical), ft	0.682
Tip chord, ft	0.318
Mean aerodynamic chord (theoretical), ft	0.522
Area (theoretical - does not include air ducts), sq ft	0.796
Aspect ratio	3.182
Taper ratio	0.467
Quarter-chord sweepback, deg	45
Dihedral, deg	-3.5
Incidence, deg	0
Twist	0
Airfoil section parallel to fuselage center line at 0.381-semispan station	NACA 65A005.5
Airfoil section parallel to fuselage center line at wing tip	NACA 65A003.7
Horizontal tail:	
Span (theoretical), ft	0.756
Root chord (theoretical), ft	0.341
Tip chord, ft	0.156
Mean aerodynamic chord (theoretical), ft	0.260
Length, ft	0.941
Area (theoretical), sq ft	0.188
Aspect ratio	3.06
Taper ratio	0.456
Quarter-chord sweepback, deg	45
Dihedral, deg	0
Incidence, deg	-3
Twist,	0
Airfoil section at root	NACA 65A006
Airfoil section at tip	NACA 65A004
Vertical tail:	
Span (theoretical), ft	0.496
Root chord at 1.591 inches above fuselage center line, ft	0.379
Tip chord, ft	0.167
Mean aerodynamic chord (exposed), ft	0.286
Length, ft	0.871
Area (exposed), sq ft	0.099
Aspect ratio (exposed)	1.333
Taper ratio (exposed)	0.440
Quarter-chord sweepback, deg	45
Airfoil section parallel to and 1.591 inches from fuselage center line	NACA 65A006
Airfoil section parallel to fuselage center line at tip	NACA 65A004

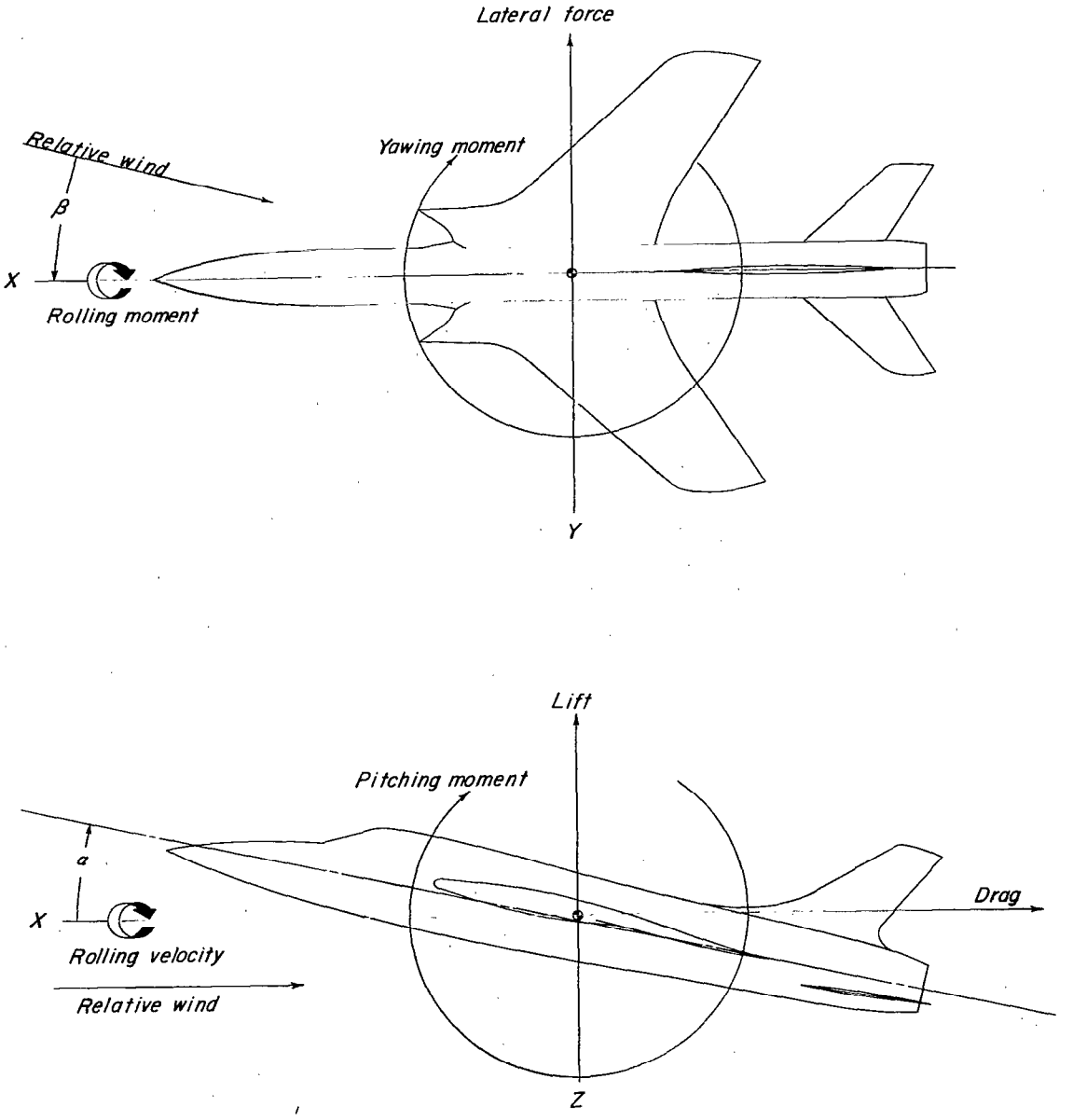

Figure 1.- System of axes used showing positive directions of forces, moments, angles, and velocities.

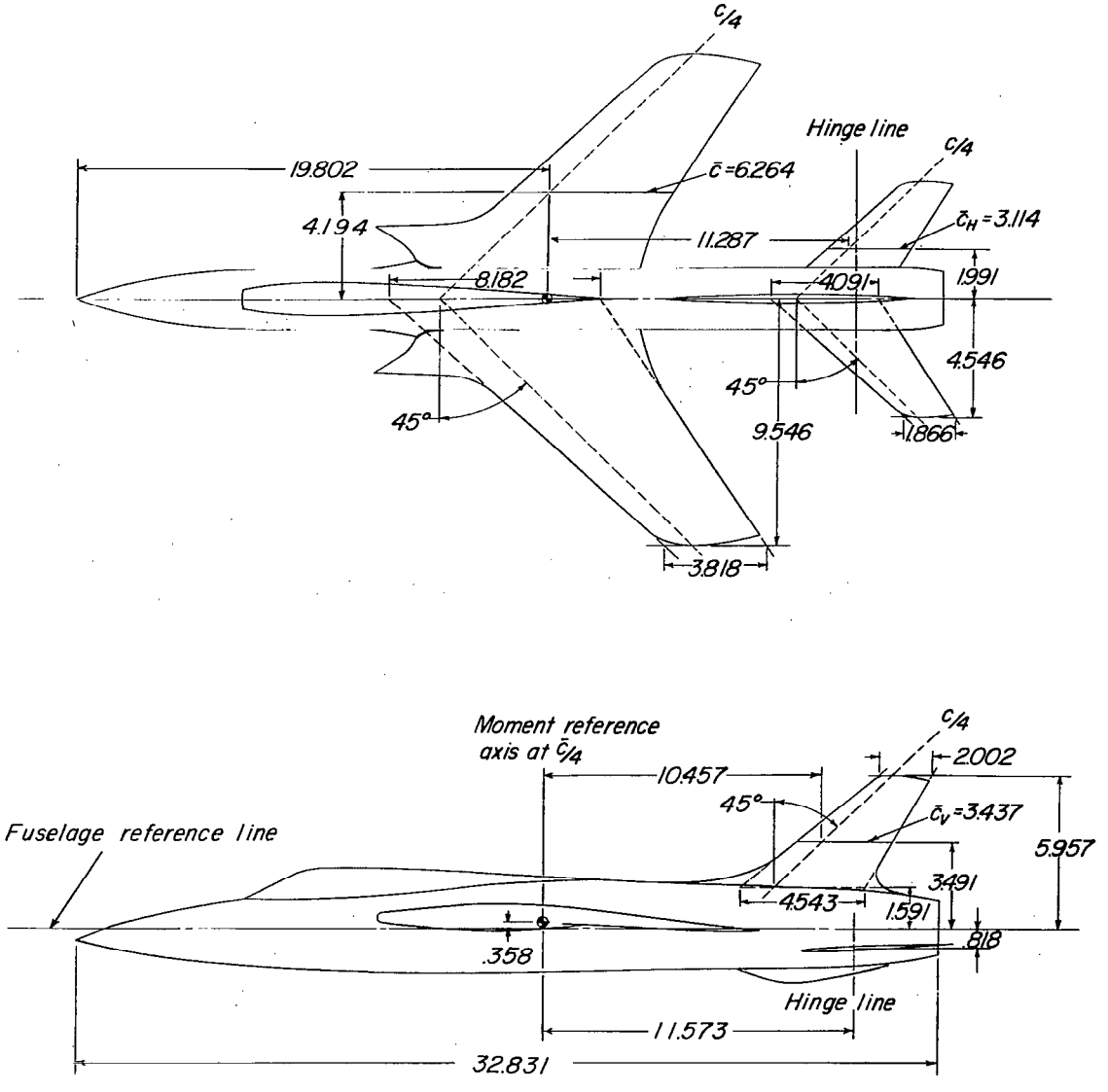

Figure 2.- Drawing of model. All dimensions are in inches unless otherwise specified.

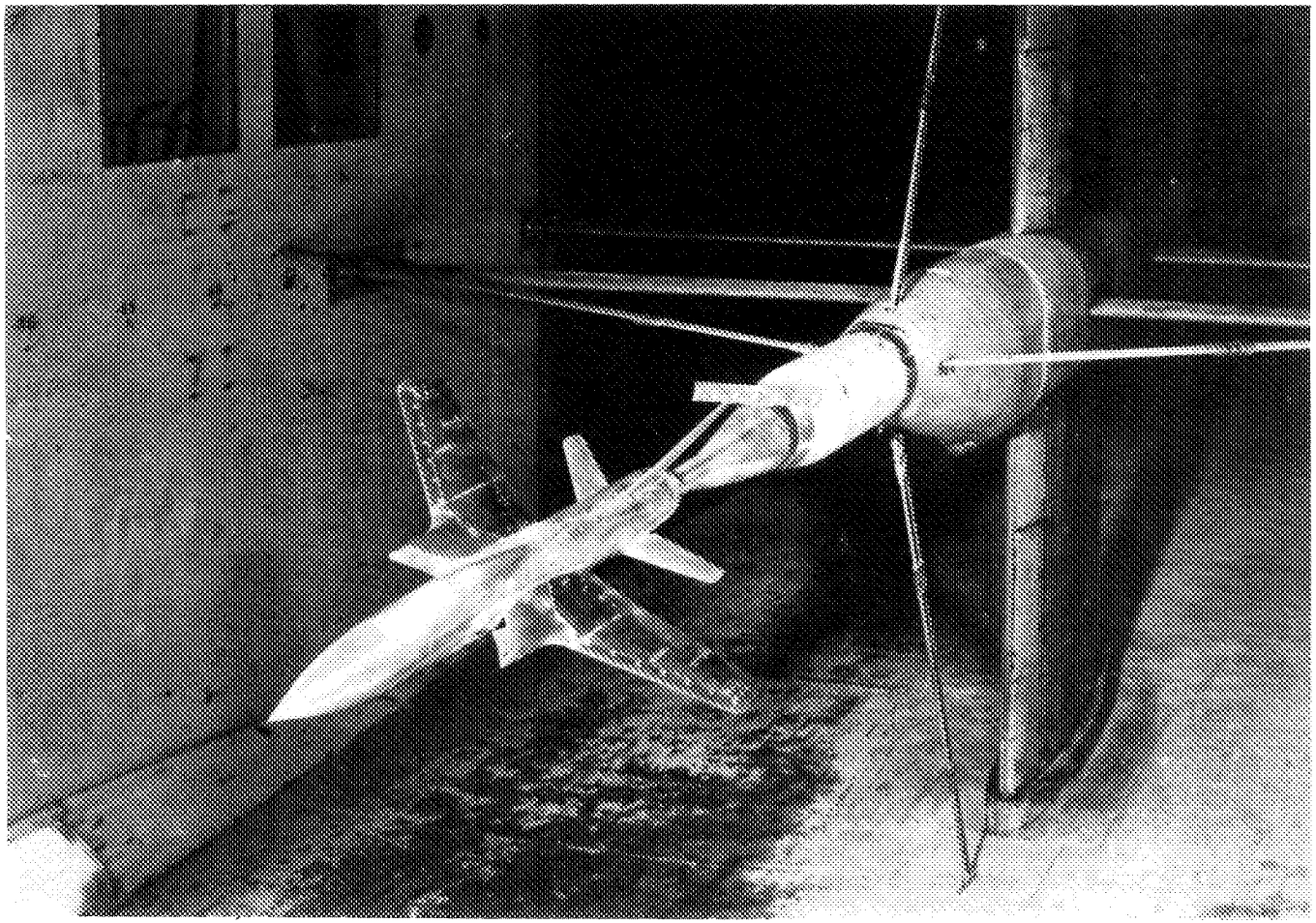

(a) $\alpha = 0^{\circ}$. L-87848

Figure 3.- Photographs of model mounted on the forced-roll support system in the Langley high-speed 7- by 10-foot tunnel.

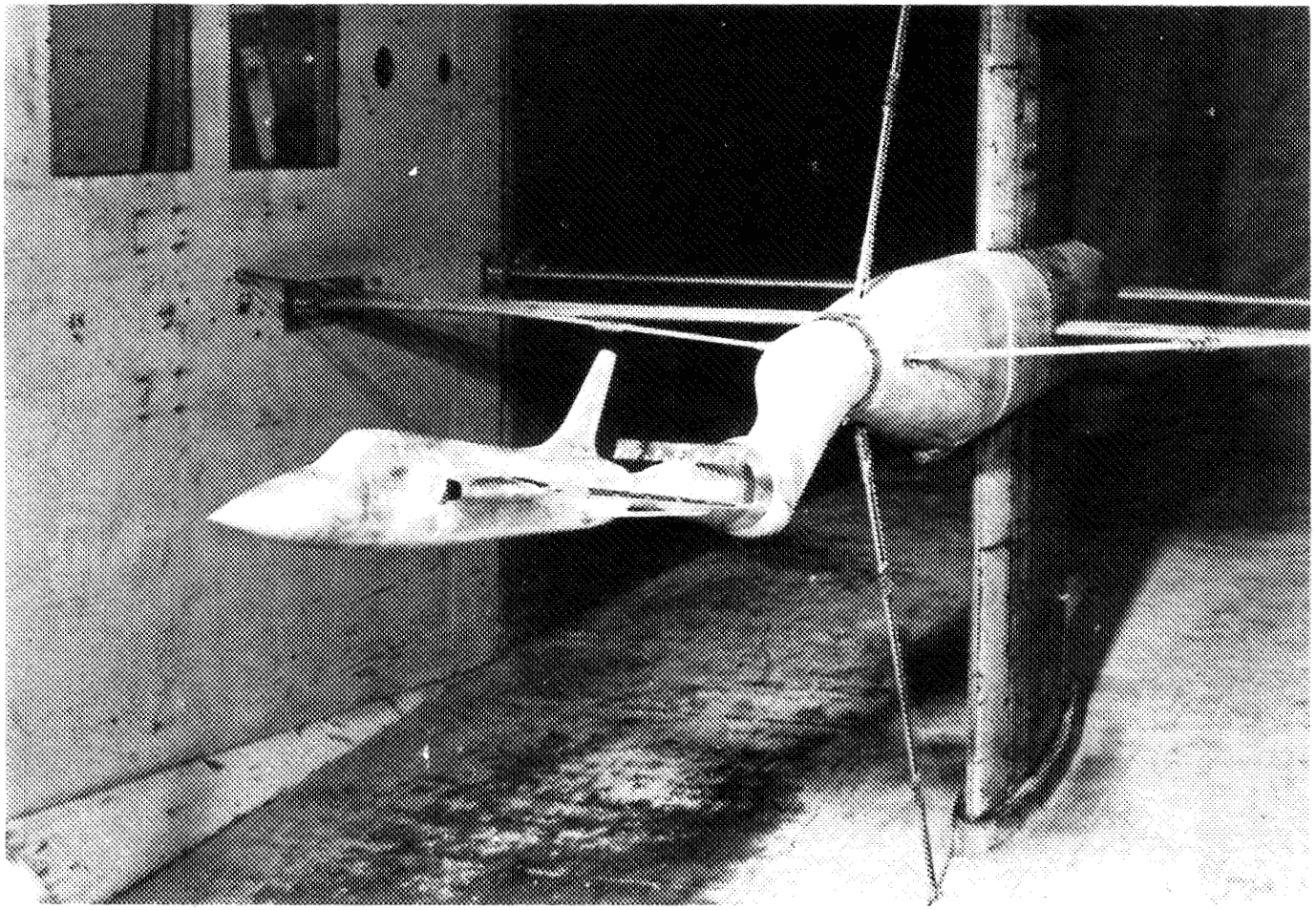

(b) $\alpha = 10^{\circ}$. L-87849

Figure 3.- Concluded.

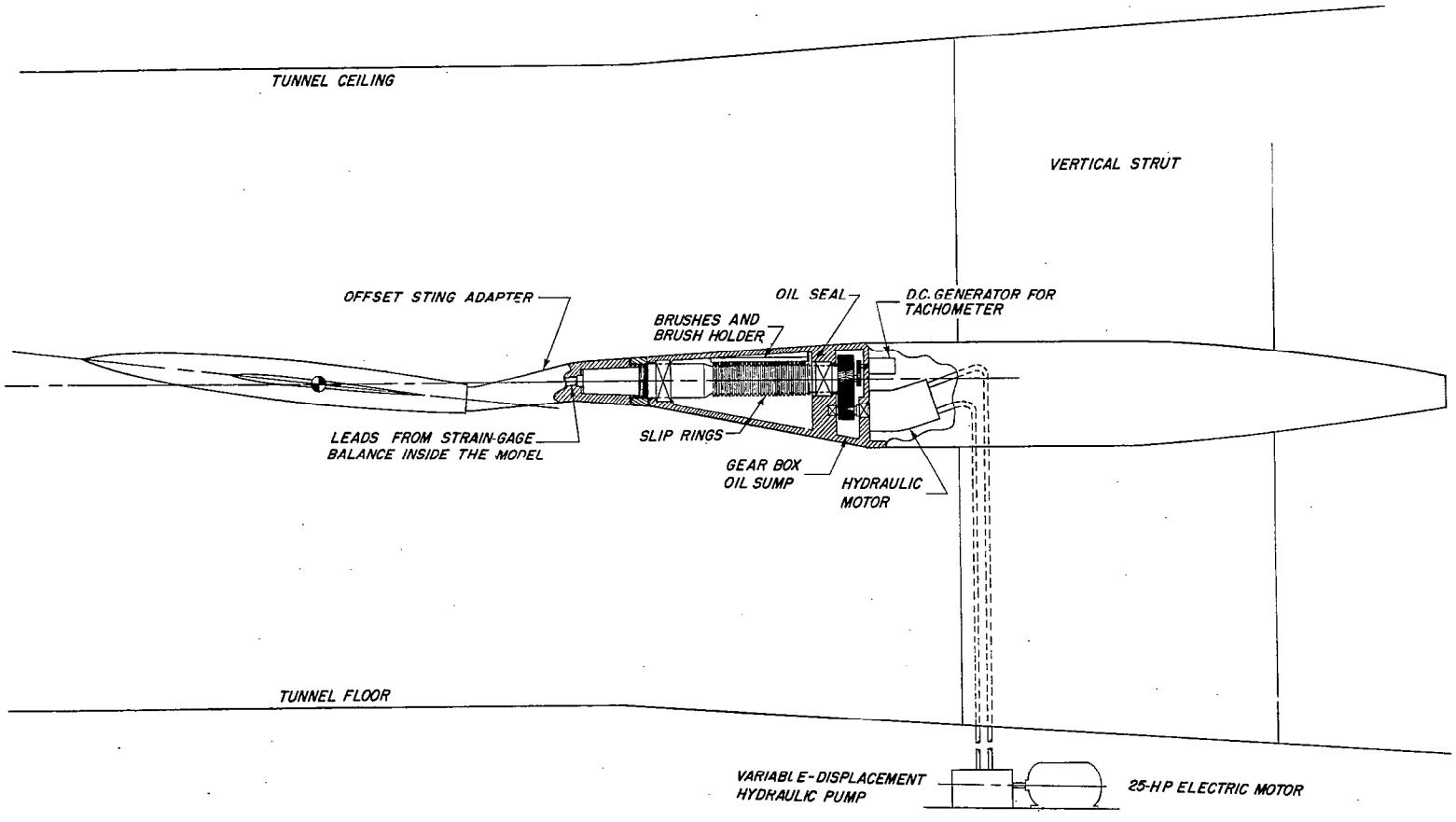

Figure 4.- General arrangement of the forced-roll support system.

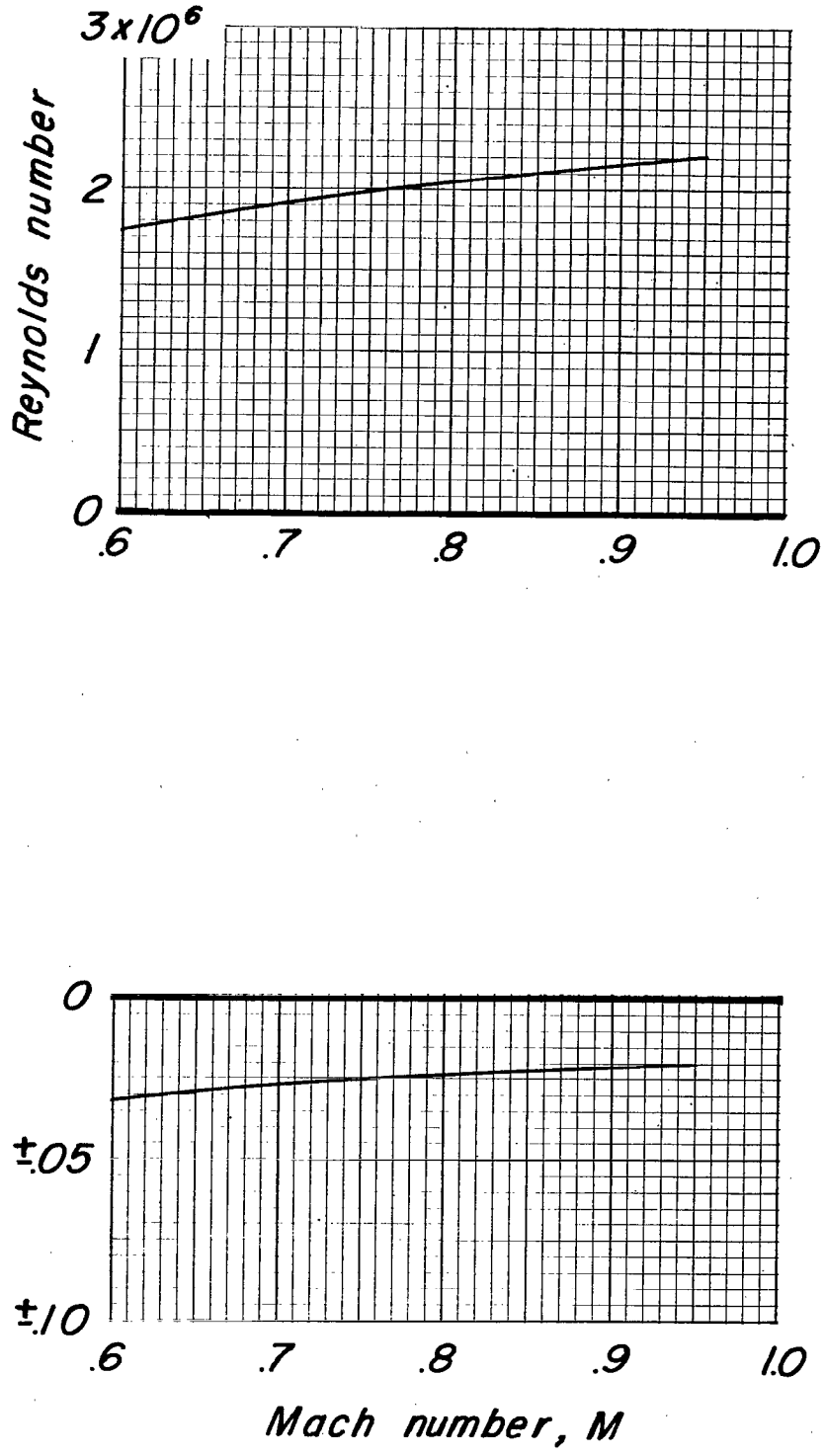

Figure 5.- Variation of test Reynolds number and maximum test pb/2V with Mach number.

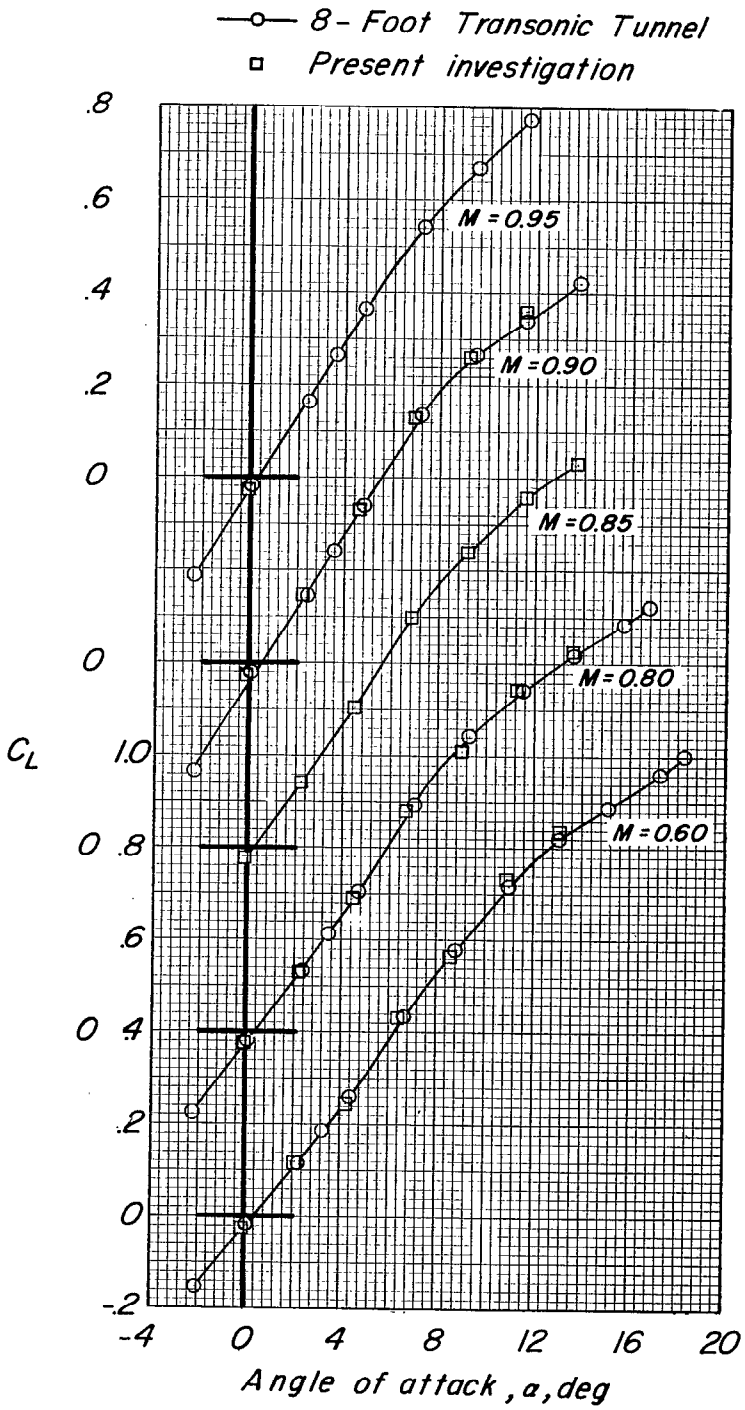

Figure 6.- Variation of lift coefficient with angle of attack for the complete-model configuration, horizontal-tail incidence = -3°. (Data of the present investigation obtained at $\frac{pb}{2V} = 0$.)

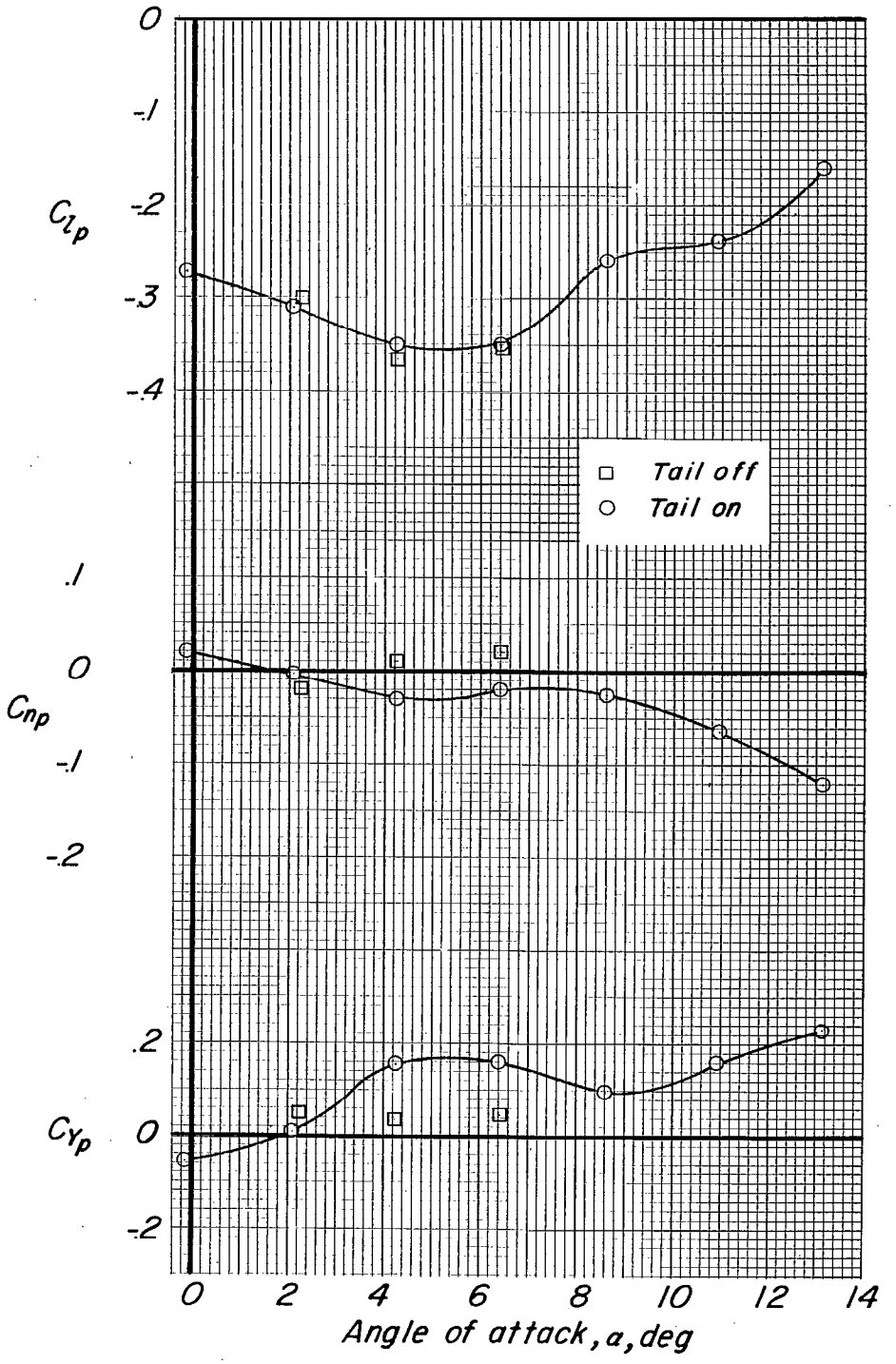

(a) M = 0.60.

Figure 7.- Variation of rolling-stability derivatives with angle of attack.

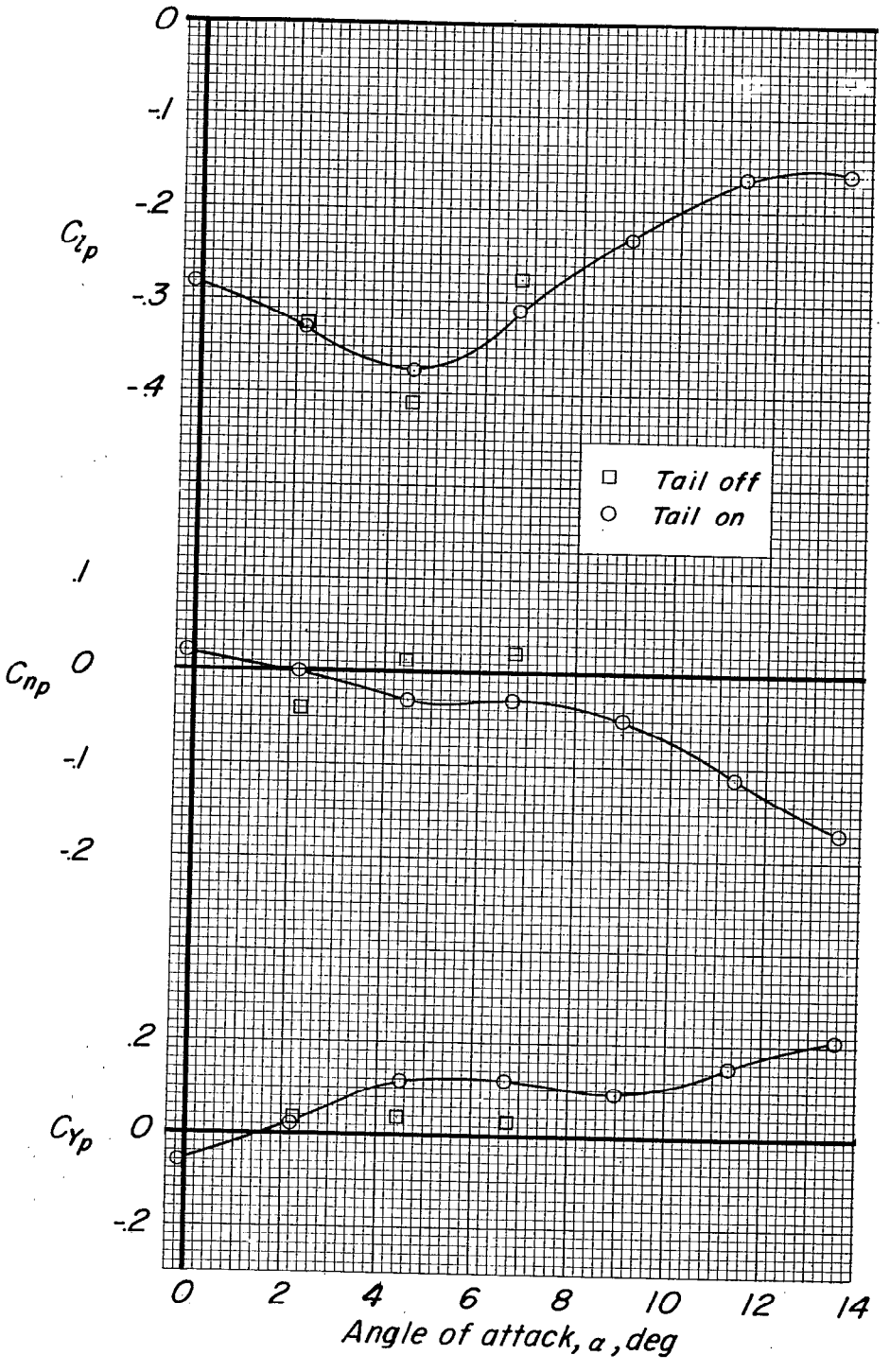

(b) M = 0.80.

Figure 7.- Continued.

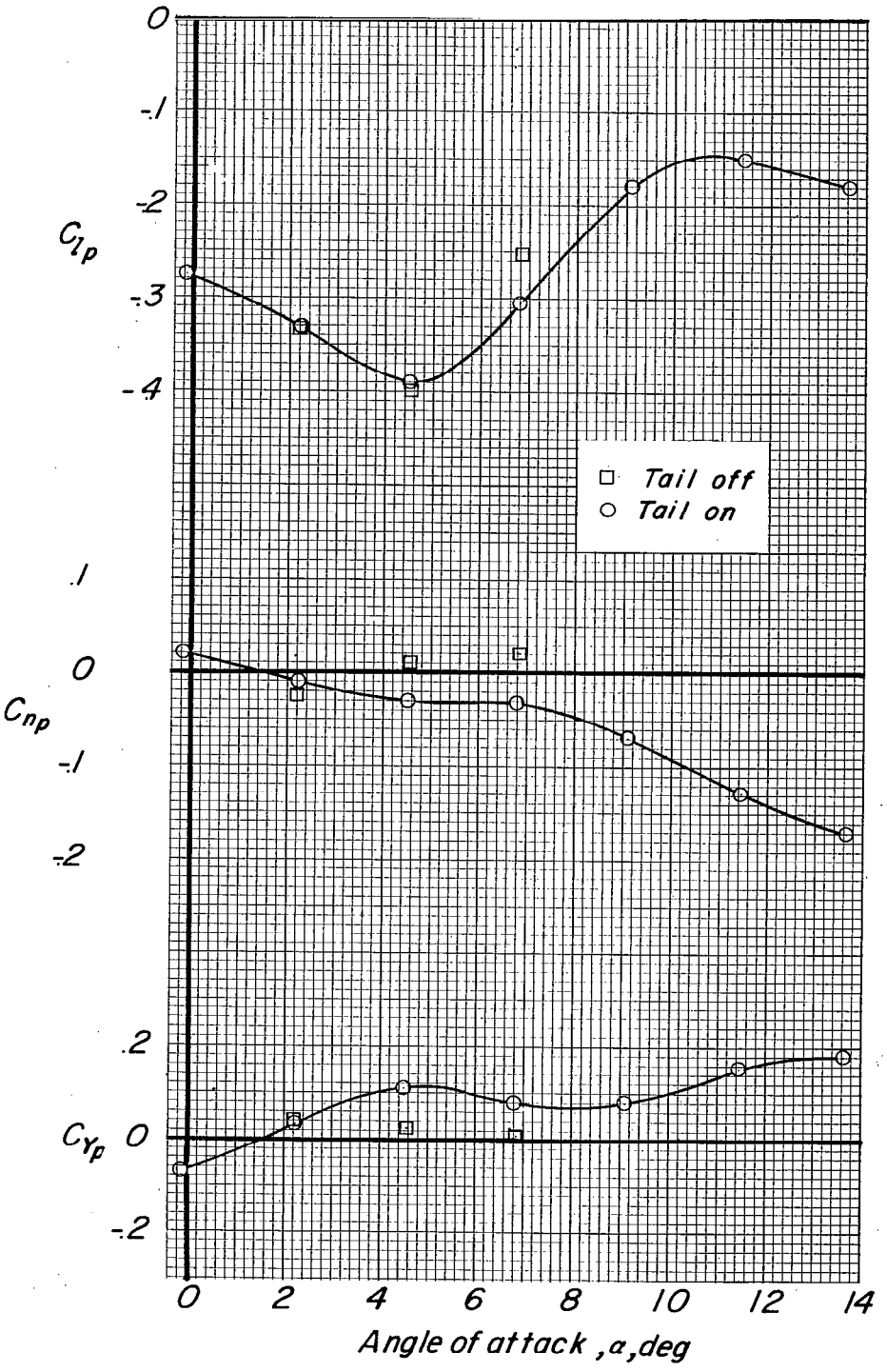

(c) M = 0.85.

Figure 7.- Continued.

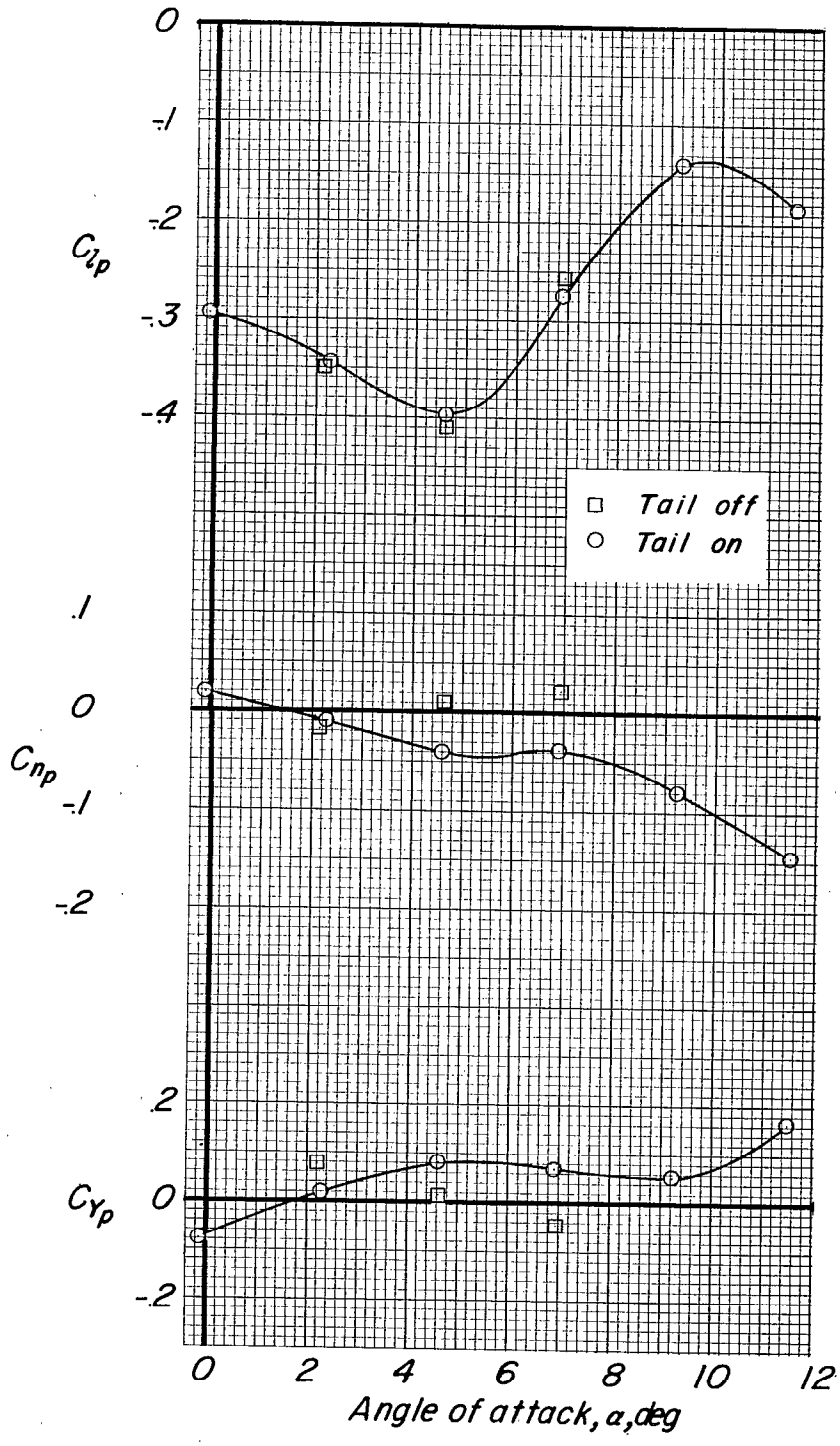

(d) M = 0.90.

Figure 7.- Continued.

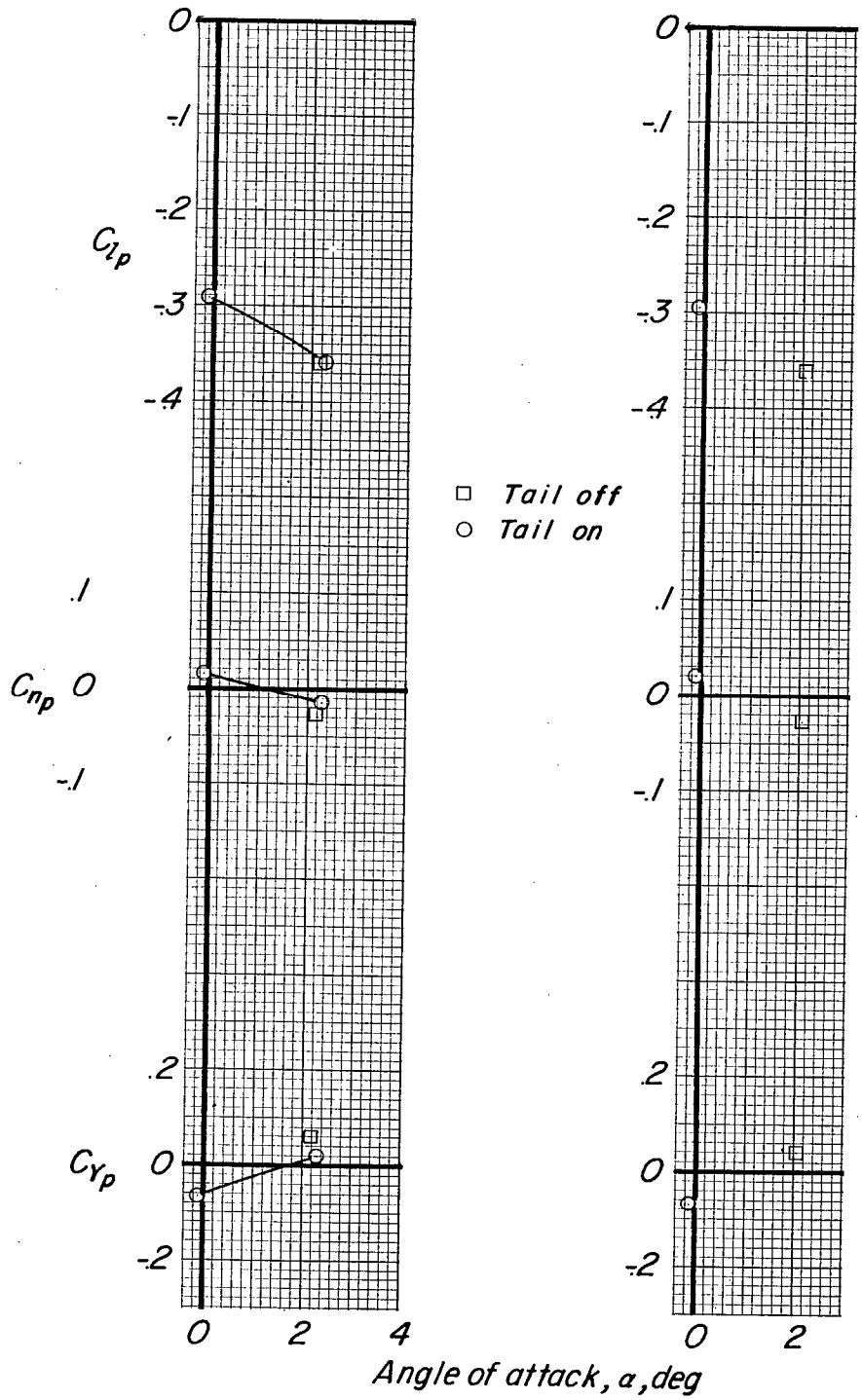

(e) M = 0.93.

(f) M = 0.95.

Figure 7.- Concluded.

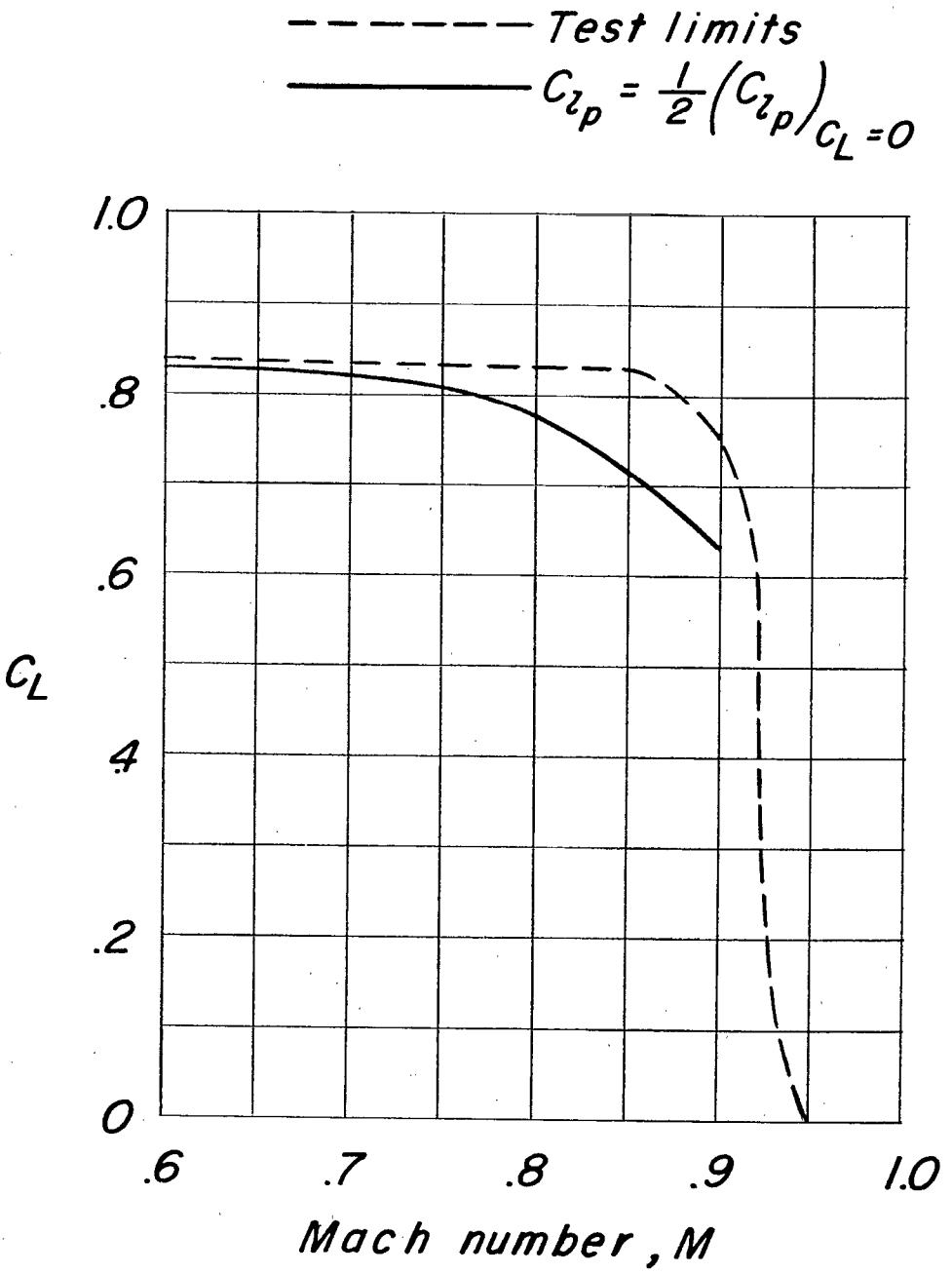

Figure 8.- Damping-in-roll boundary for the test range of lift coefficient and Mach number. (Complete-model configuration.)

CONFIDENTIAL